DNS of Shock/Boundary Layer Interaction Flow in a Supersonic Compression Ramp

Xin-Liang Li, De-Xun Fu, Yan-Wen Ma, and Xian Liang

Abstract A direct numerical simulation of the shock/turbulent boundary layer interaction flow in a supersonic 24-degree compression ramp is conducted with the free stream Mach number 2.9. The blow-and-suction disturbance in the upstream wall boundary is used to trigger the transition. Both the mean wall pressure and the velocity profiles agree with those of the experimental data, which validates the simulation. The turbulent kinetic energy budget in the separation region is analyzed. Results show that the turbulent production term increases fast in the separation region, while the turbulent dissipation term reaches its peak in the near-wall region. The turbulent transport term contributes to the balance of the turbulent conduction and turbulent dissipation. Based on the analysis of instantaneous pressure in the downstream region of the mean shock and that in the separation bubble, the authors suggest that the low frequency oscillation of the shock is not caused by the upstream turbulent disturbance, but rather the instability of separation bubble.

1 Introduction

During more than half a century study, large amount of experimental and numerical study are preformed on shock/turbulent boundary-layer interaction (STBLI), and the supersonic compression ramp flow is a typical model of STBLI [3]. Adams et al. [1] performed the first DNS of supersonic compression ramp flow. However, limited by the computing power, the Reynolds number of DNS cannot be as high as that of the experiment, and there is no direct comparison with the experiment result in the DNS used by Adam. Wu and Martin [7] performed a new DNS of supersonic compression ramp flow and the turbulence statistics agree with Bookey et al.'s experiment [2]. To minimize the computation cost, Wu and Martin used the recycler technique to produce the inlet fully developed boundary-layer turbulence. This method avoided the long computational domain for simulating the transition. However, the inlet turbulence provided by the recycler technique is not as reliable

X.-L. Li (✉)
LHD, Institute of Mechanics, CAS, Beijing 100190, China
e-mail: lixl@imech.ac.cn

A. Kuzmin (ed.), *Computational Fluid Dynamics 2010*,
DOI 10.1007/978-3-642-17884-9_93, © Springer-Verlag Berlin Heidelberg 2011

as that provided by transition simulation. This chapter has made a direct numerical simulation (DNS) of shock/turbulent boundary layer interaction (STBLI) flow in a 24-degree compression ramp with free stream Mach number 2.9. The flow parameters chosen are close to Bookey et al.'s experiment [2]. Different from Wu and Martin's simulation [7, 8], the wall blow-and-suction disturbance in the upwind wall boundary is used to trigger the transition. Based on the analysis of instantaneous pressure in the downstream region of the mean shock and that in the separation bubble, the authors suggest that the low frequency oscillation of the shock is not caused by the upstream turbulent disturbance, but rather the instability of separation bubble. The turbulent kinetic energy budget in the separation region is also analyzed in this chapter.

2 DNS Setup

As shown in Fig. 1, the computing model is supersonic flow over a 24-degree ramp, and the computational domain is also shown in this figure as the dashed line. The computational domain is $0 \leq z \leq 14\,\text{mm}$ in the spanwise direction. In the current simulation, we first simulate the two-dimensional laminar flow over a flat-plate with the leading edge, then, use the profiles of density, velocities and temperature at the 200 mm downstream leading edge are used as the inlet boundary conditions of the three-dimensional simulation. To trigger the transition, we impose the blow-and-suction perturbation on the wall at $-305\,\text{mm} \leq x \leq -285\,\text{mm}$. The Amplitude of the perturbation is set as $A = 0.1$. Table 1 shows the free-stream conditions and the condition at the location $x = -30\,\text{mm}$, which is in the upstream of the separation bubble, where θ, δ and C_f denote the momentum thickness, nominal thickness (99%) and skin friction coefficient at $x = -30\,\text{mm}$. The parameters of Bookey et al.'s experiment [2] is also listed in this table.

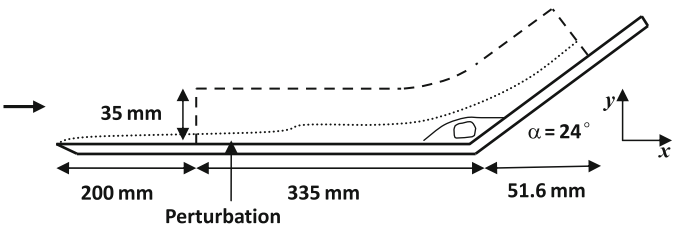

Fig. 1 Schematic diagram of DNS setup

Table 1 Flow parameters

	Free-stream and wall					$x = -30\,\text{mm}$		
	Ma_∞	$\text{Re}_\infty/\text{mm}$	T_∞/K	T_w/K	Re_θ	C_f	θ/mm	δ/mm
The current DNS	2.9	5,581.4	108.1	307	2,344	2.57×10^{-3}	0.42	6.5
Bookey et al. [2]	2.9	5,581.4	108.1	307	2,400	2.25×10^{-3}	0.43	6.7

The Navier–Stokes equations in the curvilinear-coordinate are used in the current DNS study. Steger–Warming splitting is used for the inviscid terms and then solved by using WENO-SYMBO method of Wu and Martin [7, 8]. Viscous terms are discretized by using the eighth order central scheme, and the third order TVD-type Runge–Kutta method is used for time-advance. Mesh of the current DNS is 2160 (streamwise) $\times 140$ (wall-normal) $\times 160$ (spanwise). And the mesh is concentrated in the corner region ($-35\,\text{mm} \leq x \leq 35\,\text{mm}$). The mesh span in the wall unit (measured at $x = -30\,\text{mm}$) is $\Delta x^+ \approx 4.1$, $\Delta y_w^+ \approx 0.5$ and $\Delta z^+ \approx 4.8$, which is much smaller than the DNS of non-separated flat-plate boundary layer.

3 Data Validation

Figure 2 shows the mean wall pressure $\bar{p}_w/p_\infty$ as a function of x/δ, where δ is the nominal boundary layer thickness at $x = -30\,\text{mm}$. This figure shows that the mean pressure grows rapidly in the region $x/\delta \geq -3.5$, and then forms a platform region. The circles in Fig. 2 denote the experimental data of Bookey et al. [2], and the error bar is set at 5%, and this figure shows that the current DNS result is agrees well with the experimental data. Figure 3 shows the mean velocity profile at $x = -20\,\text{mm}$, which is agrees the experimental data well. Figures 2, 3 validate the current DNS.

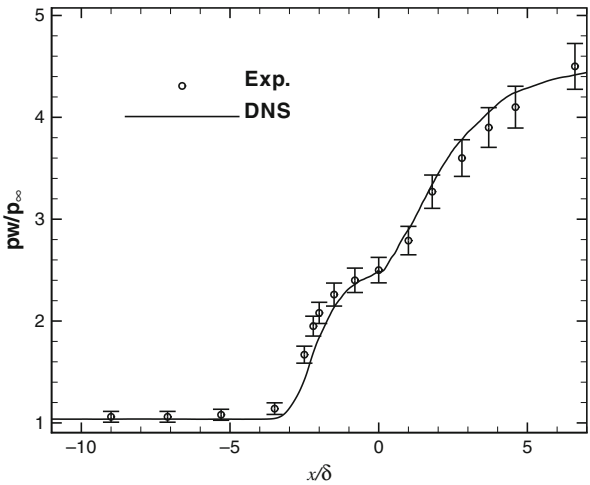

Fig. 2 Distribution of the mean wall pressure

4 Flow Visualization and Turbulent Kinetic Energy Budget

Figure 4 shows the two-dimensional distribution of the instantaneous temperature in the spanwise middle section ($z = 7\,\text{mm}$). Regions of laminar flow, transition, fully developed turbulence and separation are shown clearly in this figure. Figure 5 shows

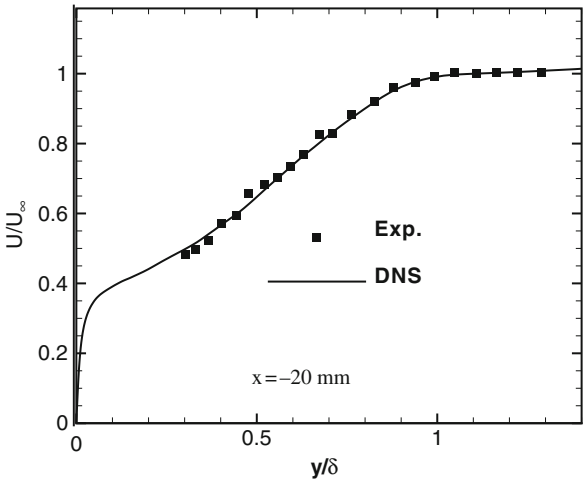

Fig. 3 Mean velocity profile at $x = -20$ mm

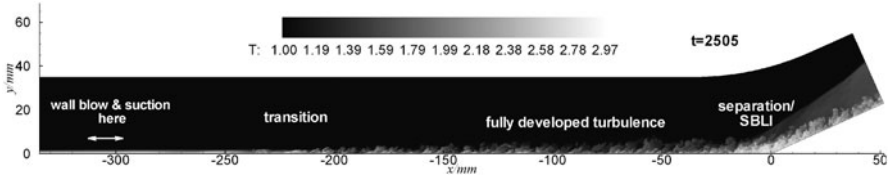

Fig. 4 Distribution of the instantaneous temperature in the middle section: $z = 7$ mm

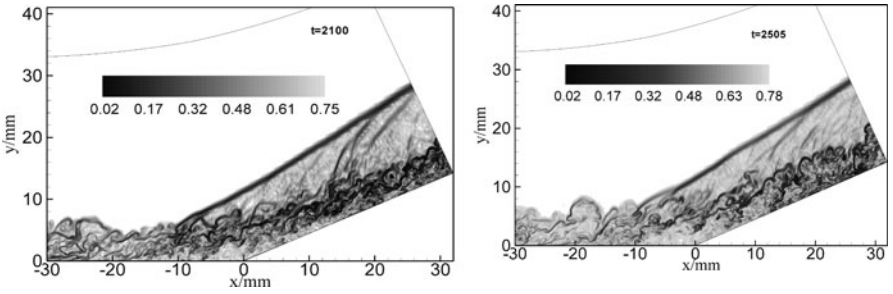

Fig. 5 Instantaneous numerical schlieren plot at $t = 2{,}100$ and $t = 2{,}505$

the instantaneous numerical schlieren plots [7] at $t = 2{,}100$ and $t = 2{,}505$, and this figure shows that the deformation of the main shock and the shocklets extends out from the boundary layer.

Figure 6 shows the two-dimensional distribution of each terms in turbulent kinetic budget [6], which contains the production term (P), dissipation term (ε), turbulent transport term (T) and pressure-dilatation term (Pdiv). This figure shows

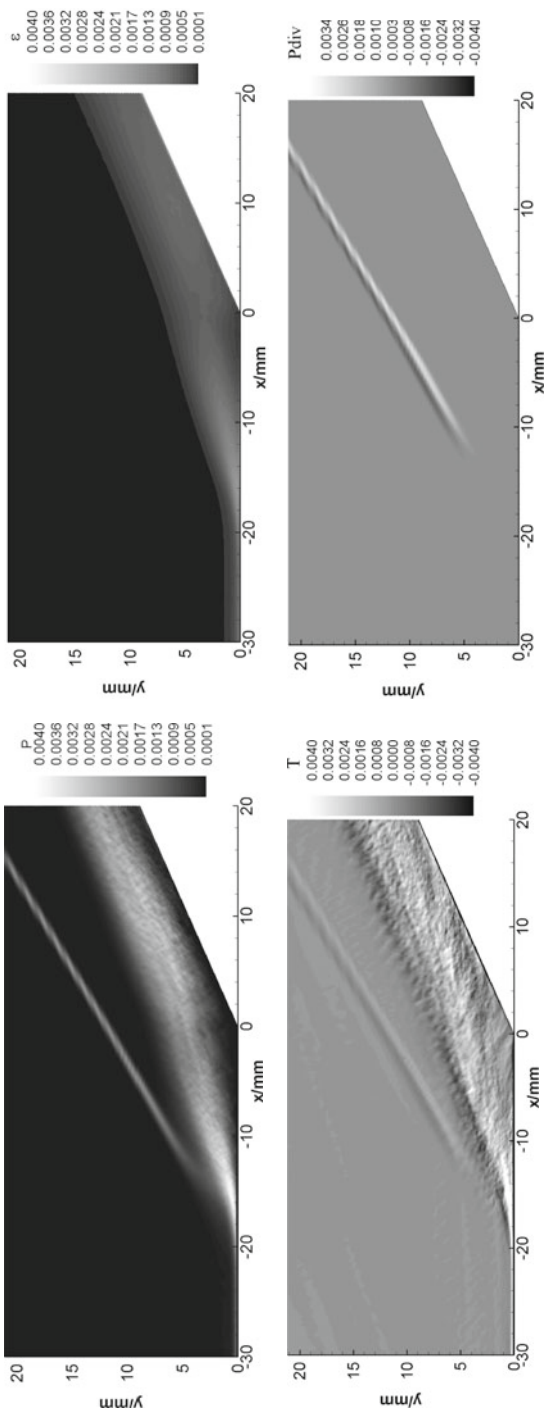

Fig. 6 Distribution of the production term (P), the dissipation term (ε), the turbulent transport (T) and the pressure-dilatation term (Pdiv) in the turbulent kinetic energy equation

that the production term is very strong in the downstream region of the separation point and in the region around the main shock. This is because the mean shear is very strong in these regions. The turbulent dissipation ε is very strong both in the separation region and the downstream near-wall region. Turbulent transport term balances the production and dissipation, and the turbulent kinetic energy is transported to the near wall region and then dissipated. This figure also shows that the pressure-dilatation term (Pdiv) is significant in the region around the main shock, while this term is ignorable in other regions. This indicates that the intrinsic compressibility effect is not significant in the region which does not contain the main shock.

5 Preliminary Investigation of the Mechanism for Shock Oscillation

The oscillation of the separation shock is an important feature of the shock/turbulent boundary layer interaction (STBLI). There are two different characteristic frequencies of the shock oscillation, and the time scale of the high-frequency oscillation is $O(\delta/U_\infty)$, while the time scale of the low-frequency one is $O(10\delta/U_\infty - 100\delta/U_\infty)$ [4]. Ganapathisubramani et al. [5] have found that there are clusters of coherent structures (so-called "super-structures") in the turbulent boundary layer and deemed that the clusters of coherent structures play an important role in the low-frequency oscillation of the shock.

Figure 7 shows the visualization of coherent structures by using the iso-surface of the second invariant of velocity gradient tensor Q. This figure shows that coherent structures are randomly arranged, and the package of coherent structures are not clear. The authors tend to believe that the package (or cluster) of the coherent structures are not the reason for the low-frequency oscillation of the shock.

Figure 8 shows the time history of pressure disturbance $p' = (p - \bar{p})/p_\infty$ in the point $(x, y) = (-9, 5.9)$, which is located in the downstream region of the shock, and the fluctuation of p' denotes the oscillation of the shock. The dash and the solid lines in Fig. 8 denote the instantaneous and filtered values of p', respectively. This figure shows that low-frequency oscillation has the time scale of

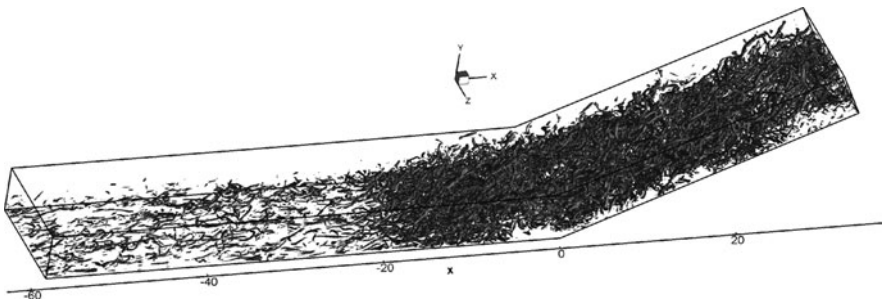

Fig. 7 Visulazation of the coherent structures (isosurface of Q)

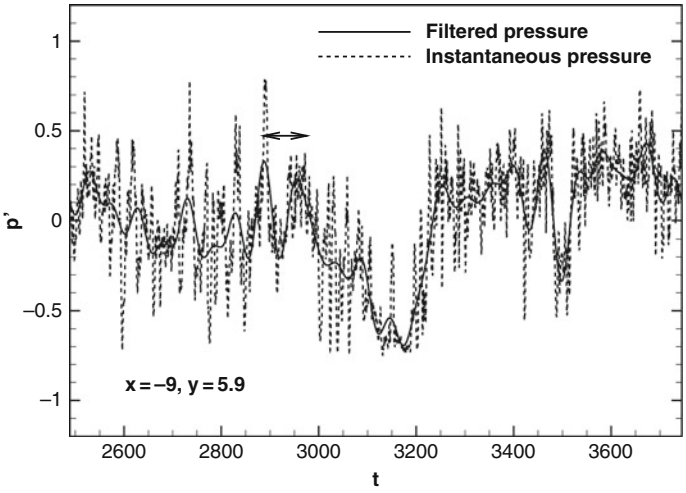

Fig. 8 Time history of the pressure disturbance at the location $(x, y) = (-9, 5.9)$

100–400 non-dimensional time units, which is approximately 15–60 times of δ/U_∞. Figure 9 shows the pressure disturbance p' at the wall at $x = -12$ mm, which is located in the separation bubble, and it also shows the oscillation with two different frequencies. The low frequency oscillation denotes the oscillation of the separation bubble, and the time scale is close to that of the shock oscillation. So, the authors conjecture that the low-frequency oscillation of the shock is associated with the oscillation of the separation bubble, and less related to the upstream coherent structures. To further validate this speculation, we perform a laminar simulation of the

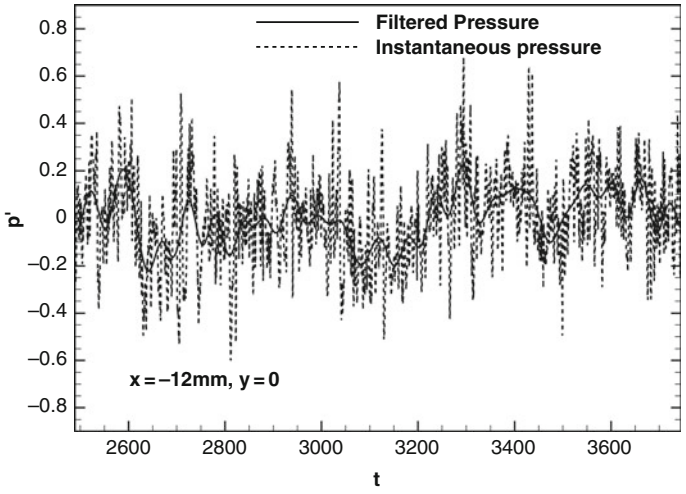

Fig. 9 Time history of the pressure disturbance at the wall of $x = -12$ mm

compression ramp flow. The laminar simulation is two-dimensional with the same free-stream conditions as the current DNS, and the geometry is also the same as the current DNS (in the x–y section). Different from the three-dimensional simulation, no perturbation is used in the two-dimensional simulation and the flow remains laminar. Figure 10 shows the instantaneous pressure in the wall at $x = -4$ mm, and this figure shows that the oscillation of wall pressure has two different time scales. The low frequency oscillation has the time scale of 400 non-dimensional time units, which is close to the time scale of low-frequency oscillation in the turbulent case. In the laminar simulation, the flow in the upstream region of the separation bubble is "clean", and there are no coherent structures or super-structures. However, the low-frequency oscillation of the separation bubble still exists. This indicates that the low-frequency oscillation is not related to the upstream disturbance. So, the authors suggest that the low frequency oscillation of the shock has little relation with the upstream turbulent disturbance, and the instability of separation bubble is the suggested reason. The mechanism of low-frequency oscillation will be further investigated in the follow-up study.

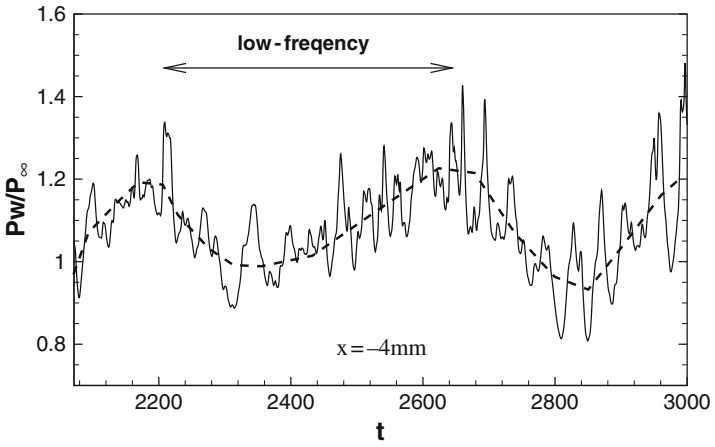

Fig. 10 Time history of the pressure disturbance at the wall of $x = -4$ mm (laminar simulation)

6 Conclusion

The direct numerical simulation of shock/turbulent boundary layer interaction flow in a supersonic compression ramp is conducted with free stream Mach number 2.9 and 24-degree ramp-angle. The upstream wall blow-and-suction perturbation is used to trigger the transition. Both the mean wall pressure and the velocity profiles agree with those of experimental data, which validates the simulation. The turbulent kinetic energy budget in the separation region is analyzed, and the mechanism of the main shock's low-frequency oscillation is also studied.

The authors suggest that the low frequency oscillation of the shock has little relation with the upstream turbulent disturbance, which results from the instability of separation bubble.

The turbulent production term increases fast in the separation bubble, while the turbulent dissipation term reaches its peak in the near-wall region. The turbulent transport term contributes to the balance of the turbulent conduction and turbulent dissipation.

References

1. Adams, N.A.: Direct simulation of the turbulent boundary layer along a compression ramp at M = 3 and Re = 1685. J. Fluid Mech. **420**, 47–83 (2000)
2. Bookey, P.B., Wyckham, C., Smits, A.J., Martin, M.P.: New Experimental Data of STBLI at DNS/LES Accessible Reynolds Numbers. AIAA Paper 2005-309 (2005)
3. Dolling, D.S.: Fifty years of shock-wave/boundary-layer interaction research: what next? AIAA J. **39**(8), 1517–1531 (2001)
4. Dolling, D.S., Or, C.T.: Unsteadiness of the shock wave structure in attached and separated compression ramp flows. Exp. Fluids **3**, 24–32 (1985)
5. Ganapathisubramani, B., Clemens, N.T., Dolling, D.S.: Low-frequency dynamics of shock-induced separation in a compression ramp interaction. J. Fluid Mech. **636**, 397–425 (2009)
6. Pirozzoli, S., Grasso, F.: Direct numerical simulation of impinging shock wave/turbulent boundary layer interaction at $M = 2.25$. Phys. Fluids **18**(6), 065113 (2006)
7. Wu, M., Martin, M.P.: Direct numerical simulation of shockwave and turbulent boundary layer interaction induced by a compression Ramp. AIAA J. **45**, 879–889 (2007)
8. Wu, M., Martin, M.P.: Analysis of shock motion in shockwave and turbulent boundary layer interaction using direct numerical simulation data. J. Fluid Mech. **594**, 71–83 (2008)